

Horizontal winds at
Rothera

R. E. Hibbins et al.

Seasonal variations in the horizontal wind structure from 0–100 km above Rothera station, Antarctica (67° S, 68° W)

R. E. Hibbins¹, J. D. Shanklin¹, P. J. Espy¹, M. J. Jarvis¹, D. M. Riggin²,
D. C. Fritts², and F.-J. Lübken³

¹Physical Sciences Division, British Antarctic Survey, High Cross, Madingley Road, Cambridge, CB3 0ET, UK

²Colorado Research Associates, 3380 Mitchell Lane, Boulder, CO 80301, USA

³Leibniz-Institute of Atmospheric Physics, Schloss-Str. 6, 18225, Kühlungsborn, Germany

Received: 2 May 2005 – Accepted: 23 May 2005 – Published: 1 July 2005

Correspondence to: R. E. Hibbins (rehi@bas.ac.uk)

© 2005 Author(s). This work is licensed under a Creative Commons License.

Title Page

Abstract

Introduction

Conclusions

References

Tables

Figures

◀

▶

◀

▶

Back

Close

Full Screen / Esc

Print Version

Interactive Discussion

EGU

Abstract

A medium frequency spaced-antenna radar has been operating at Rothera station, Antarctica (67° S, 68° W) for two periods, between 1997–1998 and since 2002, measuring winds in the mesosphere and lower thermosphere. In this paper monthly mean winds are derived and presented along with three years of radiosonde balloon data for comparison with the HWM-93 model atmosphere and other high latitude southern hemisphere sites. The observed meridional winds are slightly more northwards than those predicted by the model above 80 km in the winter months and below 80 km in summer. In addition, the altitude of the summer time zero crossing of the zonal winds above the westward jet is overestimated by the model by up to 8 km. These data are then merged with the wind climatology obtained from falling sphere measurements made during the PORTA campaign at Rothera in early 1998 and the HWM-93 model atmosphere to generate a complete zonal wind climatology between 0 and 100 km as a benchmark for future studies at Rothera. A westwards (eastwards) maximum of 44 ms⁻¹ at 67 km altitude occurs in mid December (62 ms⁻¹ at 37 km in mid July). The 0 ms⁻¹ wind contour reaches a maximum altitude of 90 km in mid November and a minimum altitude of 18 km in January extending into mid March at 75 km and early October at 76 km.

1. Introduction

The polar mesosphere and lower thermosphere is strongly coupled to the stratosphere and troposphere below by tides and upward propagating gravity waves. This coupling drives the mean circulation to states far removed from radiative equilibrium, and understanding the extent and degree of this coupling is vital to quantifying the main contributions to the energy and momentum budget of this region of the atmosphere. Rothera station is ideally situated for such studies on the Antarctic Peninsula at the edge of the wintertime polar vortex. Previous studies from Rothera have looked at the height of

Horizontal winds at Rothera

R. E. Hibbins et al.

Title Page

Abstract

Introduction

Conclusions

References

Tables

Figures

◀

▶

◀

▶

Back

Close

Full Screen / Esc

Print Version

Interactive Discussion

**Horizontal winds at
Rothera**R. E. Hibbins et al.

[Title Page](#)[Abstract](#)[Introduction](#)[Conclusions](#)[References](#)[Tables](#)[Figures](#)[◀](#)[▶](#)[◀](#)[▶](#)[Back](#)[Close](#)[Full Screen / Esc](#)[Print Version](#)[Interactive Discussion](#)

EGU

polar mesospheric clouds (Chu et al., 2004), the relationship between meridional wind and temperature in the winter mesopause (Espy et al., 2003), turbulence due to gravity waves in the mesosphere (Jones et al., 2004), the nature of the 12 h wave (Murphy et al., 2003; Riggan et al., 1999, 2003) and the temperature and horizontal wind structure in the summer mesosphere (Lübken et al., 1999, 2004).

This paper presents data from the Rothera MF radar (Jarvis et al., 1999) and radiosonde balloon launches which are combined with those from the Rothera PORTA rocket campaign in order to modify the HWM-93 model atmosphere zonal wind field above Rothera. The resulting climatology represents the mean structure of the zonal wind field from ground level to 100 km altitude.

2. Data sources

The MF profiler radar at Rothera is a coherent spaced-sensor radar system used for measuring horizontal winds in the mesosphere and lower thermosphere through the observation and analysis of D-region partial reflection echoes. The radar employs a single broad-beam transmit antenna and three spaced receive antennas in a triangular array. The radar operates at a frequency of 1.98 MHz with a transmitter power of 25 kW and full width half maximum pulse width of 25 μ s. This corresponds to a height resolution of \sim 4 km sampled at 2 km height intervals between 50 and 100 km, with the majority of echoes returned from altitudes between 75 and 95 km.

The system utilizes a full correlation analysis (Briggs, 1984; Holdsworth and Reid, 1995) to determine the wind field across the range of observations. A total of 1398 full or partial days of data recorded between 23 February 1997 and 31 December 2004 are included in this study.

A routine radiosonde program of between 2 and 4 launches per week has operated at Rothera since early 2002. Launches are normally timed for the 12:00 UT main synoptic hour, however, during the winter of 2003, balloons were launched for a special ozonesonde campaign at non standard times to obtain “matches” with other Antarctic

**Horizontal winds at
Rothera**R. E. Hibbins et al.

[Title Page](#)[Abstract](#)[Introduction](#)[Conclusions](#)[References](#)[Tables](#)[Figures](#)[I◀](#)[▶I](#)[◀](#)[▶](#)[Back](#)[Close](#)[Full Screen / Esc](#)[Print Version](#)[Interactive Discussion](#)

EGU

stations. The radiosonde system at the station uses Vaisala RS80 GPS radiosondes in conjunction with an MW15 processor, which processes the GPS signal to produce 1 min mean winds from near the surface to balloon burst, which is typically at around 20 km altitude. The balloons normally rise at $\sim 4.5 \text{ ms}^{-1}$. The results presented here include data recorded from 339 balloon launches between 22 February 2002 and 8 November 2004, of which 87% were launched between 10:00 and 14:00 UT.

The falling sphere technique, and the PORTA rocket campaign at Rothera in early 1998 have been extensively described elsewhere (Schmidlin, 1991; Lübken et al., 1999, 2004). Horizontal winds between 35 and 80 km are derived from high-precision radar tracking of the descent of a 1 m metalized mylar sphere released from a rocket at a typical altitude of 110 km. A total of 26 rocket launches were undertaken at Rothera between 4 January and 27 February 1998 (75% of which were launched within 2 h of local noon, 16:33 UT, to minimise tidal influence from one launch to the next) and the monthly mean zonal wind reproduced here is taken from the climatology derived from these observations published in Lübken et al. (2004).

Figure 1 summarises the data coverage from all sources used in this study, showing the two periods of operation of the MF radar coincident with the rocket launches in 1998 and the balloons in 2002–2004.

3. Data analysis

3.1. MF radar

Zonal and meridional wind data for each height range between 64 and 98 km were binned into half hourly means. These half hourly means were then combined into daily running three-day segments to which a 12 and 24 h sine wave and mean bias were fitted. Thus, a mean wind and a 12 and 24 h tidal phase and amplitude were calculated for each day of operation to separate the mean background wind from the tidal influence. Three-day periods with less than one third of available data (48 half

**Horizontal winds at
Rothera**R. E. Hibbins et al.

[Title Page](#)[Abstract](#)[Introduction](#)[Conclusions](#)[References](#)[Tables](#)[Figures](#)[◀](#)[▶](#)[◀](#)[▶](#)[Back](#)[Close](#)[Full Screen / Esc](#)[Print Version](#)[Interactive Discussion](#)

EGU

hourly means) were excluded from the fitting process to reduce the number of spurious data points. Individual three-day mean winds were then combined to give a mean wind for each calendar month of operation. The standard deviation was determined from the spread of data recorded each month at each height bin and typically ranged from 2 ms⁻¹ in the summer at high altitudes to as high as 20 ms⁻¹ at low altitudes in winter.

3.2. Radiosondes

Wind speed and direction data from each successful balloon flight was converted into zonal and meridional components and averaged into 1 km altitude bins between 0 and 21 km (the maximum height reached by 50% of the balloons). These were then combined by calendar month into monthly mean wind components with variability calculated from the standard deviation for all the mean measurements made in each height bin for a given month. These monthly standard deviations are typically 8 ms⁻¹, but range from 2 ms⁻¹ to a maximum of 18 ms⁻¹ at around 8 km altitude in wintertime.

3.3. Falling spheres

January and February mean zonal winds for each 1 km height bin between 35 and 70 km were calculated by averaging the climatology published in tenths of a month in Lübken et al. (2004). Errors were taken from the quoted RMS deviation from the fit increasing linearly from 4 ms⁻¹ at 35 km to 10 ms⁻¹ at 70 km.

4. Mean winds

Rothera monthly mean zonal and meridional winds recorded between 0 and 21 km and 63 and 99 km are reproduced in Fig. 2. In the mesosphere and lower thermosphere the main features of the data are a strong reversal of the zonal jet below 85 km from a summertime westward maximum of 44 ms⁻¹ in mid December to a wintertime eastward maximum of 40 ms⁻¹ in early July. The wintertime eastward zonal jet lessens

**Horizontal winds at
Rothera**R. E. Hibbins et al.

[Title Page](#)[Abstract](#)[Introduction](#)[Conclusions](#)[References](#)[Tables](#)[Figures](#)[◀](#)[▶](#)[◀](#)[▶](#)[Back](#)[Close](#)[Full Screen / Esc](#)[Print Version](#)[Interactive Discussion](#)

EGU

with height to around 10 ms^{-1} at 95 km altitude. The same applies to the summertime westward jet, which undergoes a westward to eastward reversal around 87 km continuing to a maximum of 15 ms^{-1} eastward at 95 km. The meridional winds are generally much weaker than the zonal winds. In wintertime the meridional wind is southward (up to 15 ms^{-1}) at low altitudes, reverses its direction around 75 km and reaches 10 ms^{-1} northwards at 95 km. In summer the meridional winds are northwards (10 ms^{-1}) between 75 and 90 km and fall to around zero above and below this.

Rothera is at a similar latitude to several stations where long term observations of winds in the mesosphere and lower thermosphere have been undertaken allowing comparison of longitudinally distinct sites. At Mawson station (67° S , 63° E) the summertime westwards to eastwards wind reversal occurs significantly higher than that observed at Rothera, ranging from 100 km in October to 90 km in March (Portnyagin et al., 1993). The wintertime eastward wind is slightly stronger ($10\text{--}15 \text{ ms}^{-1}$) at Mawson between 80 and 98 km than that observed at Rothera ($5\text{--}10 \text{ ms}^{-1}$). The meridional winds at Mawson and Rothera are very similar with the only notable difference occurring in March where the meridional wind turns southwards ($5\text{--}10 \text{ ms}^{-1}$) at Mawson between 80 and 100 km, a feature not observed in the Rothera data. The zonal wind at 95 km altitude at Molodezhnaya (68° S , 45° E) varies between 20 ms^{-1} eastwards in the winter and 12 ms^{-1} westwards in November (Portnyagin et al., 1993). At Rothera the winds at the same altitude are eastwards all year between 15 ms^{-1} in summer down to $<5 \text{ ms}^{-1}$ around the equinoxes, and the zonal wind reversal between October and December at Molodezhnaya is not seen at Rothera. The corresponding meridional wind at Molodezhnaya is northward ($0\text{--}5 \text{ ms}^{-1}$) around the equinoxes as seen at Rothera, but at mid winter turns southwards ($5\text{--}10 \text{ ms}^{-1}$) and strongly northwards (15 ms^{-1}) in mid summer, the opposite of the behaviour observed at Rothera at 95 km. Finally, the mean zonal winds observed at Davis (69° S , 78° E) and Syowa (69° S , 40° E) are very similar (Dowdy et al., 2001, 2004; Kishore et al., 2003). At 80 km altitude both sites see a reversal of the mean wind field in mid March and early October as seen at Rothera. The winter time eastward jet at Syowa and Davis is between 10 and 20 ms^{-1} at 80 km,

**Horizontal winds at
Rothera**R. E. Hibbins et al.

[Title Page](#)[Abstract](#)[Introduction](#)[Conclusions](#)[References](#)[Tables](#)[Figures](#)[◀](#)[▶](#)[◀](#)[▶](#)[Back](#)[Close](#)[Full Screen / Esc](#)[Print Version](#)[Interactive Discussion](#)

EGU

slightly stronger than that observed at Rothera, and the westward summer time jet at Davis and Syowa is also around 10 ms^{-1} stronger than at Rothera.

Müllemann and Lübken (2004) have presented a summertime zonal wind climatology from Andøya rocket range (69° N , 16° E) between 35 and 80 km based on falling sphere data gathered over 125 rocket flights. Comparison between this and the Rothera zonal winds over the common range of altitudes shows that in the southern hemisphere the westwards maximum wind occurs much earlier in the summer and at a much lower altitude than at a comparable northern hemisphere latitude (67 km in mid December at Rothera compared to above 80 km in mid August at Andøya). The autumn westward to eastward wind reversal occurs at a similar time of year at each site (~ 80 days after solstice at 70 km altitude) although the rate at which the wintertime eastwards wind increases is much greater in the northern hemisphere, e.g. at 70 km altitude the wind increases from 0 to 25 ms^{-1} within 20 days at Andøya whereas 20 days after the autumn zero crossing at Rothera the 70 km zonal wind is only 15 ms^{-1} eastwards.

Between 0 and 21 km the wintertime zonal winds increase eastwards with increasing altitude reaching a maximum of 40 ms^{-1} at 21 km in August. In summer the low altitude zonal winds are light ($< 10 \text{ ms}^{-1}$) eastwards. In general the monthly zonal winds are less variable in the lower stratosphere than they are in the troposphere, except in late winter and spring. At this time the station is sometimes inside and sometimes outside the strong circumpolar vortex. This strong winter circulation usually begins to break down in late October or early November, and by late December a generally stagnant summer circulation is in place. The vortex then begins to build again during the autumn. The meridional winds are southwards ($< 10 \text{ ms}^{-1}$) in summer and late winter/spring reversing northwards ($< 15 \text{ ms}^{-1}$) in autumn and late spring.

5. Comparison with HWM-93

Figures 3 and 4 show the monthly mean meridional and zonal winds recorded with the MF radar and radiosonde balloon launches for comparison with the HWM-93 model at-

**Horizontal winds at
Rothera**R. E. Hibbins et al.

[Title Page](#)[Abstract](#)[Introduction](#)[Conclusions](#)[References](#)[Tables](#)[Figures](#)[I◀](#)[▶I](#)[◀](#)[▶](#)[Back](#)[Close](#)[Full Screen / Esc](#)[Print Version](#)[Interactive Discussion](#)

EGU

mosphere (Hedin et al., 1996). There is a tendency for the mean observed meridional winds to be more northwards than the HWM-93 model atmosphere winds, particularly above 80 km in winter time (April to September) and between 65 and 80 km in the summer months (November to February). The wintertime transition from poleward to equatorward meridional flow at Rothera occurs up to 15 km lower than that predicted by the model (e.g. in June, 78 km rather than 91 km). However, elsewhere the model meridional winds agree with the observational data to within natural variability and experimental uncertainty. For the zonal wind component the only point at which the model deviates significantly from the observed winds occurs at high altitudes in summertime (November to February) where the model is seen to overestimate the altitude of the maximum extent of the westward summer time zonal jet by around 6 km. Hence it overestimates the westward wind above 85 km and underestimates the wind between 65 and 80 km. In all other cases the observed winds and the model winds are in agreement.

6. Zonal wind climatology

Figure 5 shows the monthly mean zonal winds recorded with the MF radar for comparison with the falling sphere data recorded in January and February 1998 at Rothera. Where the data overlap (between 64 and 70 km) the two techniques are found to agree to within 4 ms^{-1} in January and 10 ms^{-1} in February. This agreement is within the individual errors associated with each technique at these altitudes (10 ms^{-1} for the falling spheres and $\sim 5 \text{ ms}^{-1}$ for the MF radar in summer), though both techniques show how the HWM-93 model underestimates the westward extent of the summer time zonal jet around 60 to 70 km altitude.

The two data sets were combined to give a weighted average zonal wind between 64 and 70 km for January and February. Then, in order to generate a complete zonal wind climatology below 100 km, gaps in the altitude coverage of the mean monthly data (22–34 km in January and February and 22–62 km in all other months) were filled

**Horizontal winds at
Rothera**R. E. Hibbins et al.

[Title Page](#)[Abstract](#)[Introduction](#)[Conclusions](#)[References](#)[Tables](#)[Figures](#)[◀](#)[▶](#)[◀](#)[▶](#)[Back](#)[Close](#)[Full Screen / Esc](#)[Print Version](#)[Interactive Discussion](#)

EGU

with the monthly mean zonal winds generated from the HWM-93 model. The resulting monthly wind profiles were then fitted with polynomials of increasing order until the goodness of fit (as measured by the chi squared of the polynomial fit to the data) did not significantly improve. The resulting sixth order polynomial fits to the monthly profiles, the coefficients of which are listed in Table 1, were then combined to generate the contour plot reproduced in Fig. 6 which clearly illustrates the seasonal variations in the zonal wind field from summertime westwards to wintertime eastwards flow.

A westwards maximum of 44 ms^{-1} at 67 km altitude occurs in mid December with an eastwards maximum of 62 ms^{-1} at 37 km in mid July. The 0 ms^{-1} wind contour, representing the transition from westwards to eastwards zonal flow, extends into early March at 75 km and is crossed again in early October in the transition from wintertime eastwards to summertime westwards flow. The maximum altitude of the 0 ms^{-1} contour occurs at 90 km at the beginning of November, before the summertime westward zonal jet is fully established, and then descends to 82 km by the end of February.

Figure 7 shows the difference between the Rothera monthly zonal wind climatology and the HWM-93 monthly mean zonal winds. The overestimation by the model of the height and underestimation of the extent of the summertime westward jet above Rothera is clearly visible in the difference contours with a large positive difference peaking at 90 km in December and a negative difference around 70 km in spring and summer.

7. Summary

Data from an MF radar, radiosonde balloon launches and falling sphere measurements have been used to modify the HWM-93 model to generate a new wind climatology showing the seasonal variation in the zonal wind field above Rothera station, Antarctica. Differences are observed between the modified and unmodified model particularly in the height and extent of the westwards zonal jet observed in the summertime high altitude winds. These differences are also seen in comparisons between the mean

**Horizontal winds at
Rothera**R. E. Hibbins et al.

[Title Page](#)[Abstract](#)[Introduction](#)[Conclusions](#)[References](#)[Tables](#)[Figures](#)[I◀](#)[▶I](#)[◀](#)[▶](#)[Back](#)[Close](#)[Full Screen / Esc](#)[Print Version](#)[Interactive Discussion](#)

EGU

winds observed at Rothera and those from other northern and southern hemisphere sites of similar latitude indicative of an atypical gravity wave field around Rothera. Ern et al. (2004) observe high values of gravity wave momentum flux along the Antarctic Peninsula at 25 km altitude from temperature data derived from satellite measurements. This enhancement is due mainly to a localised region of short horizontal wavelength gravity waves where the Peninsula meets the edge of the Antarctic polar vortex. Combined lidar and airglow imager studies are currently underway to further investigate the nature of the gravity wave activity at Rothera.

Acknowledgements. The authors would like to thank the staff of the Engineering and Data Management Group and of the Meteorological and Ozone Monitoring Unit of the Physical Sciences Division at the British Antarctic Survey for their technical assistance, and for the maintenance and operation of the MF radar and radiosonde system. Research support for D. C. Fritts and D. M. Riggin was provided under NSF Office of Polar Programs grant OPP-0438777.

References

- Briggs, B. H.: The analysis of spaced sensor records by correlation techniques, Handbook for Middle Atmosphere Program, 13, 1984.
- Chu, X., Nott, G. J., Espy, P. J., Gardner, C. S., Diettrich, J. C., Clilverd, M. A., and Jarvis, M. J.: Lidar observations of polar mesospheric clouds at Rothera, Antarctica (67.5° S, 68.0° W), Geophys. Res. Lett., 31, L02114, doi:10.1029/2003GL018638, 2004.
- Dowdy, A., Vincent, R. A., Igarashi, K., Murayama, Y., and Murphy, D. J.: A comparison of mean winds and gravity wave activity in the northern and southern polar MLT, Geophys. Res. Lett., 28(8), 1475–1478, 2001.
- Dowdy, A., Vincent, R. A., Murphy, D. J., Tsutsumi, M., Riggin, D. M., and Jarvis, M. J.: The large scale dynamics of the mesosphere-lower thermosphere during the Southern Hemisphere stratospheric warming of 2002, Geophys. Res. Lett., 31, L14102, doi:10.1029/2004GL020282, 2004.
- Ern, M., Preusse, P., Alexander, M. J., and Warner, C. D.: Absolute values of gravity wave momentum flux derived from satellite data, J. Geophys. Res., 109, D20103, doi:10.1029/2004JD004752, 2004.

**Horizontal winds at
Rothera**R. E. Hibbins et al.

[Title Page](#)[Abstract](#)[Introduction](#)[Conclusions](#)[References](#)[Tables](#)[Figures](#)[◀](#)[▶](#)[◀](#)[▶](#)[Back](#)[Close](#)[Full Screen / Esc](#)[Print Version](#)[Interactive Discussion](#)

EGU

Espy, P. J., Hibbins, R. E., Jones, G. O. L., Riggan, D. M., and Fritts, D. C.: Rapid, large-scale temperature changes in the polar mesosphere and their relationship to meridional flows, *Geophys. Res. Lett.*, 30(5), 1240, doi:10.1029/2002GL016452, 2003.

Hedin, A. E., Fleming, E. L., Manson, A. H., Schmidlin, F. J., Avery, S. K., Clark, R. R., Franke, S. J., Fraser, G. J., Tsuda, T., Vial, F., and Vincent, R. A.: Empirical wind model for the upper, middle and lower atmosphere, *J. Atmos. Terr. Phys.*, 58(13), 1421–1447, 1996.

Holdsworth, D. A. and Reid, I. M.: A simple model of atmospheric radar backscatter: description and application to the full correlation analysis of spaced antenna data, *Radio Sci.*, 30, 1263–1280, 1995.

Jarvis, M. J., Jones, G. O. L., and Jenkins, B.: New initiatives in observing the Antarctic mesosphere, *Adv. Space Res.*, 24(5), 611–619, 1999.

Jones, G. O. L., Clilverd, M. A., Espy, P. J., Chew, S., Fritts, D. C., and Riggan, D. M.: An alternative explanation of PMSE-like scatter in MF radar data, *Ann. Geophys.*, 22, 2715–2722, 2004,

[SRef-ID: 1432-0576/ag/2004-22-2715](#).

Kishore, P., Namboothiri, S. P., Igarashi, K., Murayama, Y., Vincent, R. A., Dowdy, A., Murphy, D. J., and Watkins, B. J.: Further evidence of hemispheric differences in the MLT mean wind climatology: Simultaneous MF radar observations at Poker Flat (65° N, 147° W) and Davis (69° S, 78° E), *Geophys. Res. Lett.*, 30(6), 1336, doi:10.1029/2002GL016750, 2003.

Lübken, F.-J., Jarvis, M. J., and Jones, G. O. L.: First insitu temperature measurements at the Antarctic summer mesopause, *Geophys. Res. Lett.*, 26, 3581–3584, 1999.

Lübken, F.-J., Müllemann, A., and Jarvis, M. J.: Temperatures and horizontal winds in the Antarctic summer mesosphere, *J. Geophys. Res.*, 109(D24), art. no. D24112, 2004.

Müllemann, A. and Lübken, F.-J.: Horizontal winds in the mesosphere at high latitudes, *Adv. Space Res.*, in press, doi:10.1016/j.ars.2004.11.014, 2004.

Murphy, D. J., Tsutsumi, M., Riggan, D. M., Jones, G. O. L., Vincent, R., Hagan, M. E., and Avery, S. K.: Observations of a nonmigrating component of the semidiurnal tide over Antarctica, *J. Geophys. Res.*, 108(D8), 4241, doi:10.1029/2002JD003077, 2003.

Portnyagin, Yu. I., Forbes, J. M., Fraser, G. J., Vincent, R. A., Avery, S. K., Lysenko, I. A., and Makarov, N. A.: Dynamics of the Antarctic and Arctic mesosphere and lower thermosphere regions-I, The prevailing wind, *J. Atmos. Terr. Phys.*, 55(6), 827–841, 1993.

Riggan, D., Fritts, D. C., Jarvis, M. J., and Jones, G. O. L.: Spatial structure of the 12-hour wave in the Antarctic as observed by radar, *Earth Planets Space*, 51, 621–628, 1999.

Riggin, D., Meyer, C. K., Fritts, D. C., Murayama, Y., Igarashi, K., Vincent, R. A., Singer, W., and Murphy, D. J.: MF radar observations of semidiurnal motions in the mesosphere at high northern and southern latitudes, *J. Atmos. Solar-Terr. Phys.*, 65, 483–493, 2003.

Schmidlin, F. J.: The inflatable sphere: A technique for the accurate measurement of middle atmosphere temperatures, *J. Geophys. Res.*, 96, 22 673–22 682, 1991.

**Horizontal winds at
Rothera**

R. E. Hibbins et al.

Title Page

Abstract

Introduction

Conclusions

References

Tables

Figures

◀

▶

◀

▶

Back

Close

Full Screen / Esc

Print Version

Interactive Discussion

Horizontal winds at Rothera

R. E. Hibbins et al.

Table 1. Coefficients for the monthly sixth order polynomial fits to the mean zonal wind in ms^{-1} at Rothera between $z=0$ and 99 km: $U(z) = \sum_{n=0}^6 A_n z^n$.

Month	A_0	A_1	A_2	A_3	A_4	A_5	A_6
Jan	-5.48944E+00	4.48684E+00	-4.85350E-01	2.04222E-02	-4.16766E-04	3.99177E-06	-1.42475E-08
Feb	-6.47381E+00	8.13806E+00	-8.90085E-01	3.66976E-02	-7.03852E-04	6.29655E-06	-2.11793E-08
Mar	-5.63122E+00	5.38167E+00	-5.57603E-01	2.25848E-02	-4.19939E-04	3.62268E-06	-1.17716E-08
Apr	-1.87528E+00	4.75221E+00	-4.61081E-01	1.93211E-02	-3.65859E-04	3.14991E-06	-1.00900E-08
May	1.61436E+00	2.71009E+00	-1.78305E-01	8.38373E-03	-1.80589E-04	1.69112E-06	-5.71783E-09
Jun	4.53522E+00	-1.51375E+00	3.11613E-01	-1.06580E-02	1.54852E-04	-1.07397E-06	2.95499E-09
Jul	2.37827E+00	2.37865E-02	2.39488E-01	-9.49083E-03	1.48828E-04	-1.09536E-06	3.17636E-09
Aug	2.72424E+00	2.94386E+00	-8.51252E-02	3.13813E-03	-8.05287E-05	8.77683E-07	-3.29349E-09
Sep	1.47295E+00	9.75392E-01	5.00225E-02	-1.13480E-03	-1.43588E-05	3.94679E-07	-1.96540E-09
Oct	-3.98911E+00	2.89396E+00	-8.18105E-02	1.23490E-03	-2.38641E-05	2.99068E-07	-1.30088E-09
Nov	-7.72034E+00	5.11481E+00	-3.80745E-01	1.38831E-02	-2.73446E-04	2.60496E-06	-9.27647E-09
Dec	-1.88589E+00	2.01708E+00	-2.00486E-01	9.12702E-03	-2.18799E-04	2.40559E-06	-9.49624E-09

[Title Page](#)
[Abstract](#)
[Introduction](#)
[Conclusions](#)
[References](#)
[Tables](#)
[Figures](#)
[Back](#)
[Close](#)
[Full Screen / Esc](#)
[Print Version](#)
[Interactive Discussion](#)

EGU

**Horizontal winds at
Rothera**

R. E. Hibbins et al.

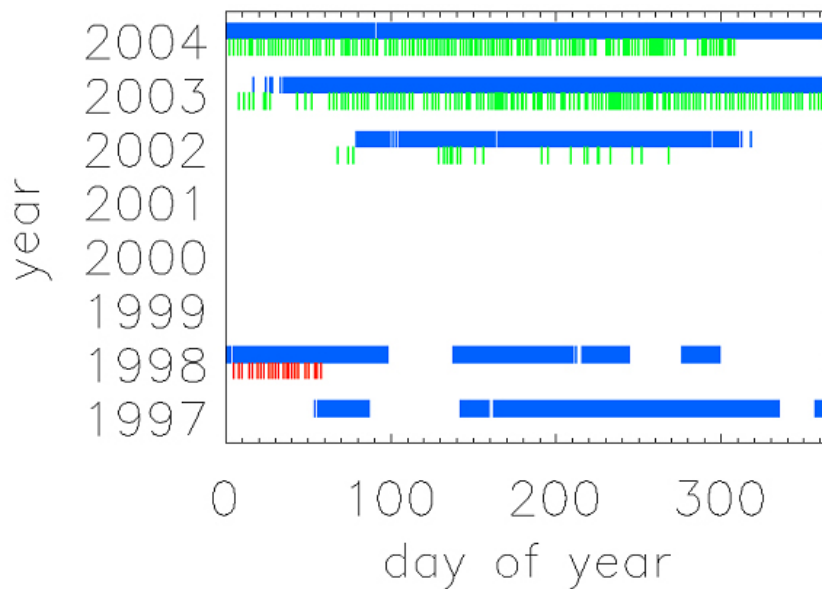


Fig. 1. Coverage of MF radar data recorded at Rothera used in this study (blue) together with falling sphere rocket launch times (red) and radiosonde balloon launch times (green).

[Title Page](#)[Abstract](#)[Introduction](#)[Conclusions](#)[References](#)[Tables](#)[Figures](#)[◀](#)[▶](#)[◀](#)[▶](#)[Back](#)[Close](#)[Full Screen / Esc](#)[Print Version](#)[Interactive Discussion](#)

EGU

**Horizontal winds at
Rothera**

R. E. Hibbins et al.

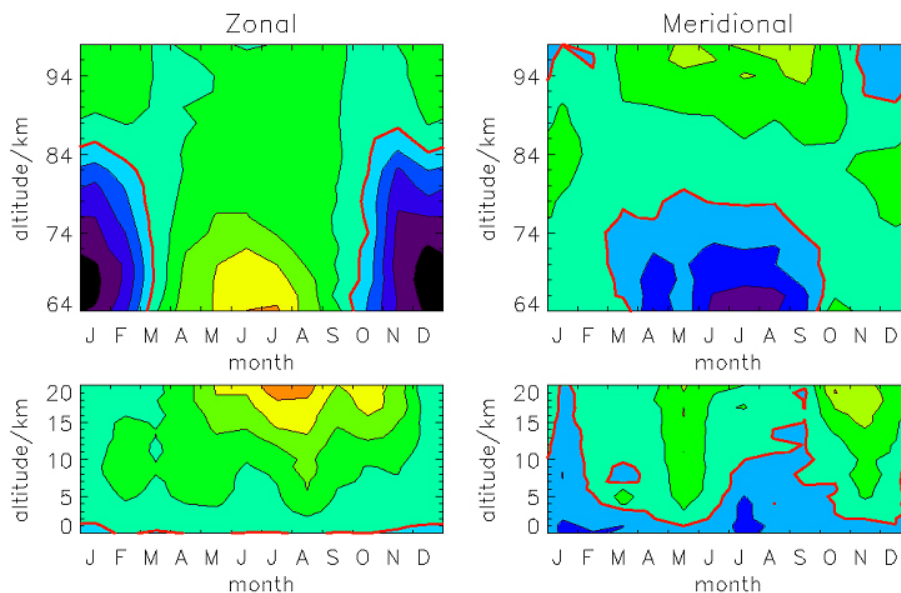


Fig. 2. Monthly mean zonal and meridional winds recorded from Rothera with the MF radar (top panels) and radiosondes (bottom panels). The thick red line represents the 0 ms^{-1} contour with other contours drawn at 10 ms^{-1} intervals for the zonal winds and 5 ms^{-1} intervals for the meridional winds (blue: westwards/southwards).

[Title Page](#)[Abstract](#)[Introduction](#)[Conclusions](#)[References](#)[Tables](#)[Figures](#)[◀](#)[▶](#)[◀](#)[▶](#)[Back](#)[Close](#)[Full Screen / Esc](#)[Print Version](#)[Interactive Discussion](#)

EGU

Horizontal winds at
Rothera

R. E. Hibbins et al.

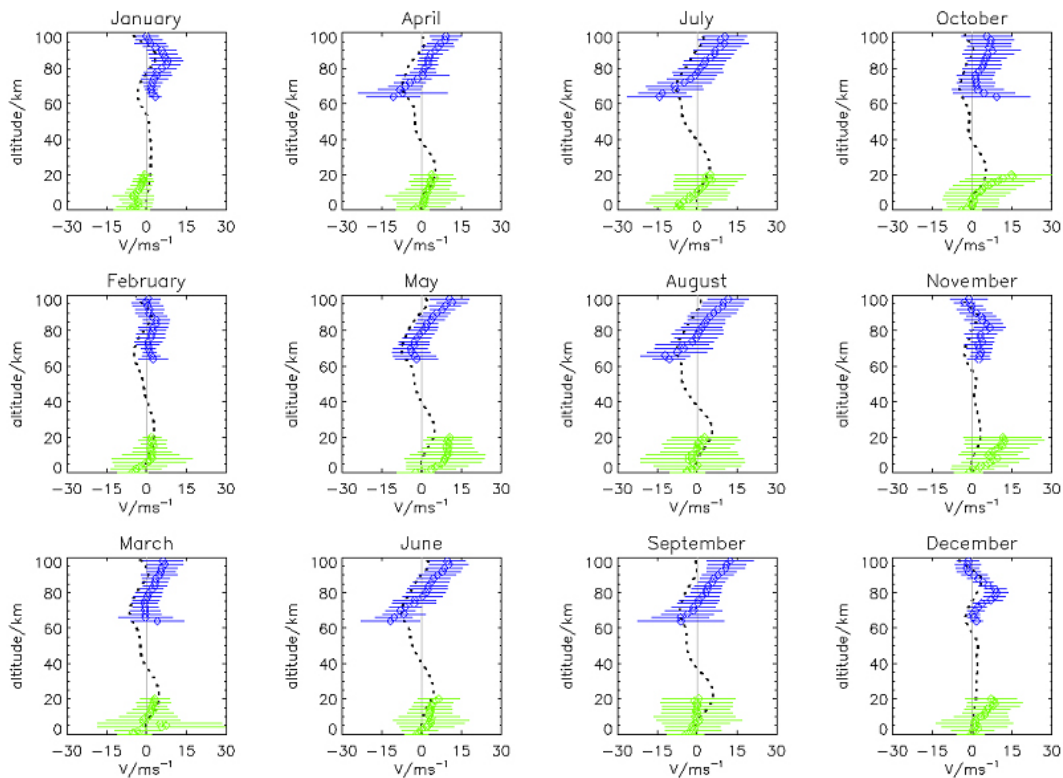


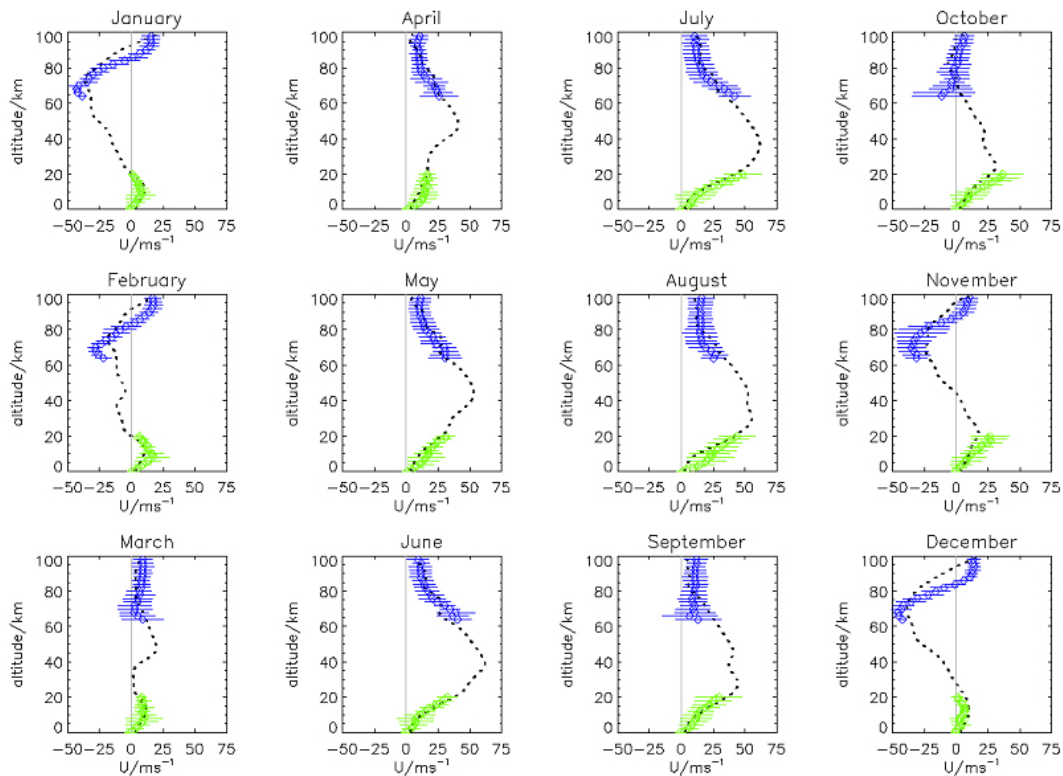
Fig. 3. Rothera monthly mean meridional winds below 100 km. Green diamonds: radiosonde data; blue diamonds MF radar winds. The dotted black line is the monthly mean HWM-93 model meridional wind for Rothera.

[Title Page](#)[Abstract](#)[Introduction](#)[Conclusions](#)[References](#)[Tables](#)[Figures](#)[◀](#)[▶](#)[◀](#)[▶](#)[Back](#)[Close](#)[Full Screen / Esc](#)[Print Version](#)[Interactive Discussion](#)

EGU

**Horizontal winds at
Rothera**

R. E. Hibbins et al.

**Fig. 4.** As Fig. 3 but for Rothera zonal winds.[Title Page](#)[Abstract](#)[Introduction](#)[Conclusions](#)[References](#)[Tables](#)[Figures](#)[◀](#)[▶](#)[◀](#)[▶](#)[Back](#)[Close](#)[Full Screen / Esc](#)[Print Version](#)[Interactive Discussion](#)

EGU

**Horizontal winds at
Rothera**

R. E. Hibbins et al.

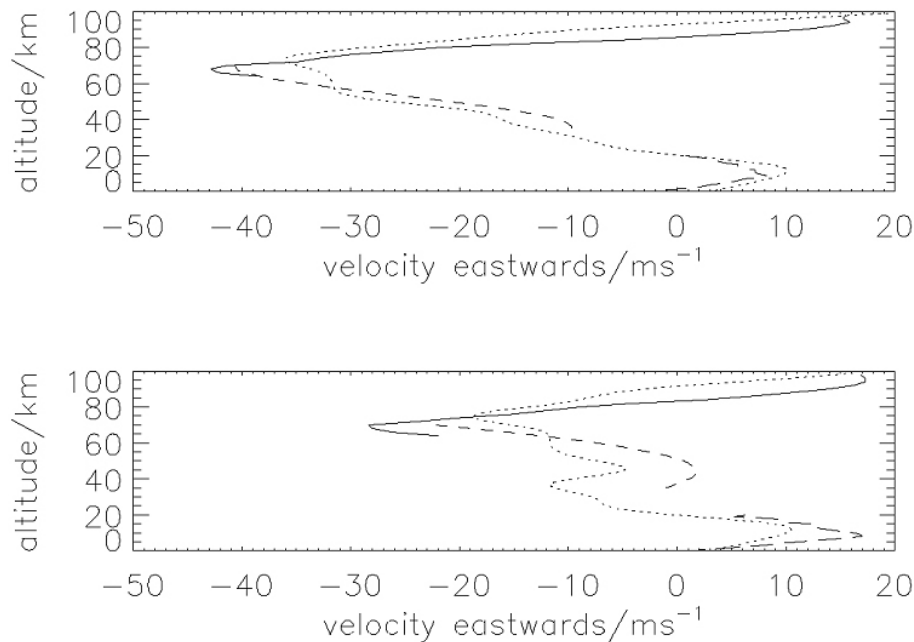


Fig. 5. Mean zonal wind recorded with the MF radar (solid line), falling spheres (short dashed line) and radiosondes (long dashed line) for January (upper panel) and February (lower panel). HWM-93 model zonal winds are shown for comparison (dotted line). Error bars (see Figs. 3 and 4) are omitted for clarity.

[Title Page](#)[Abstract](#)[Introduction](#)[Conclusions](#)[References](#)[Tables](#)[Figures](#)[◀](#)[▶](#)[◀](#)[▶](#)[Back](#)[Close](#)[Full Screen / Esc](#)[Print Version](#)[Interactive Discussion](#)

EGU

**Horizontal winds at
Rothera**

R. E. Hibbins et al.

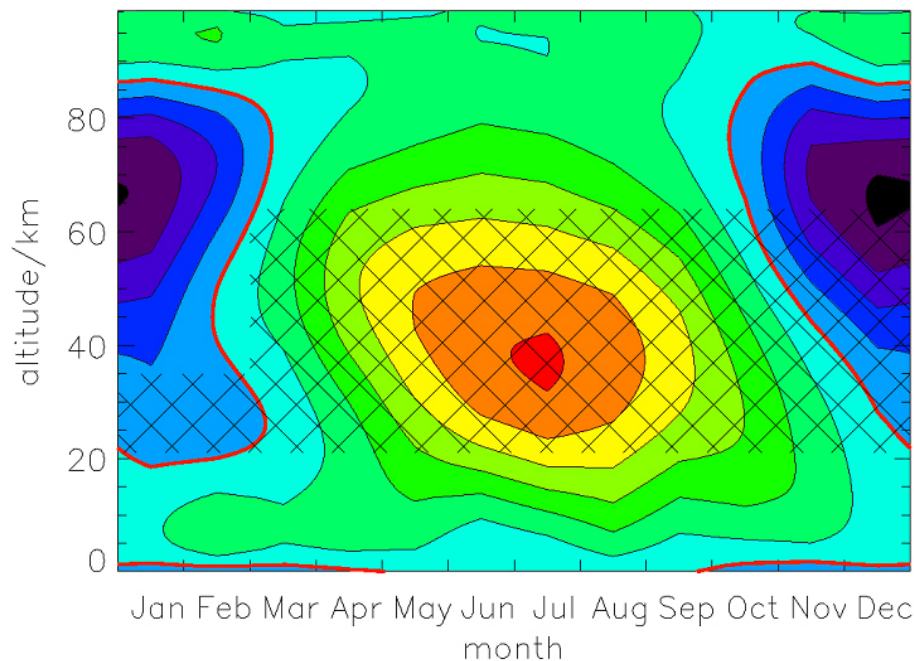


Fig. 6. Mean zonal wind above Rothera from 0–100 km. Generated from 6th order polynomial fits to the monthly mean data and, within the hatched area, monthly mean HWM-93 model winds. The thick red line represents the 0 ms^{-1} contour, other contours are drawn at 10 ms^{-1} intervals (blue: westwards).

[Title Page](#)[Abstract](#)[Introduction](#)[Conclusions](#)[References](#)[Tables](#)[Figures](#)[◀](#)[▶](#)[◀](#)[▶](#)[Back](#)[Close](#)[Full Screen / Esc](#)[Print Version](#)[Interactive Discussion](#)

EGU

**Horizontal winds at
Rothera**

R. E. Hibbins et al.

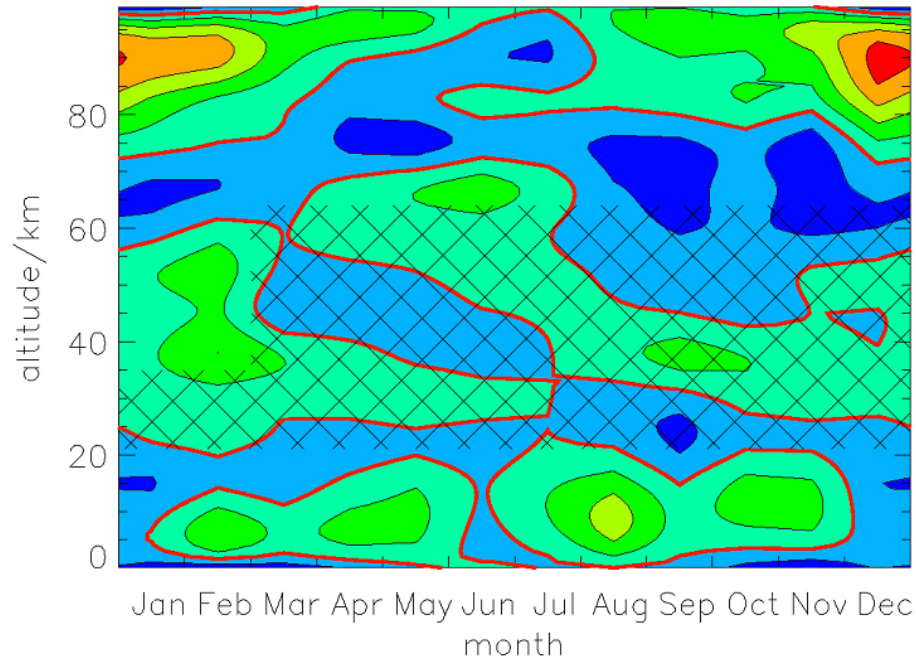


Fig. 7. Rothera zonal wind climatology (see Fig. 5) minus the HWM-93 model zonal winds. Hatched area and solid red line as in Fig. 6, contours are drawn at 5 ms^{-1} intervals (blue: negative).

[Title Page](#)[Abstract](#)[Introduction](#)[Conclusions](#)[References](#)[Tables](#)[Figures](#)[◀](#)[▶](#)[◀](#)[▶](#)[Back](#)[Close](#)[Full Screen / Esc](#)[Print Version](#)[Interactive Discussion](#)

EGU